CM13v251022wed

2025년 10월 22일 수요일 15:58

☐ Preliminaries

(i) Waterfilling procedure for parallel Gaussian channels ($\to$ frequency-selective CT channel)

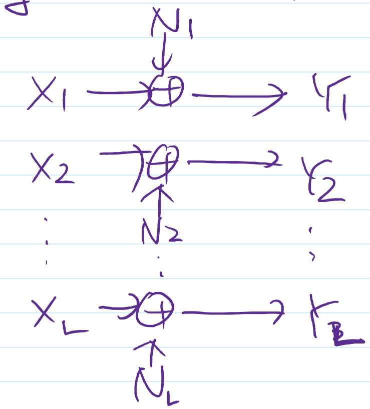

$$\sum_{i=1}^{L} E\{|X_i|^2\} \le P$$

N_i's are independent & $N_i \sim \mathcal{CN}(0, \sigma_i^2)$, $\sigma_i^2 > 0, \forall i$

$$\max_{f_{\underline{X}}(\underline{x})} I(\underline{X};\underline{Y})$$

$$\text{s.t. } \sum_{i=1}^{L} E\{|X_i|^2\} \le P$$

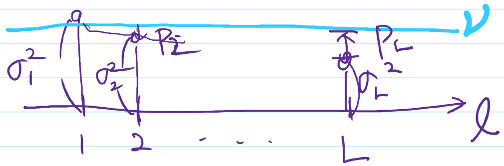

$$\sum_{i=1}^{L} [\nu - \sigma_i^2]^+ = P$$

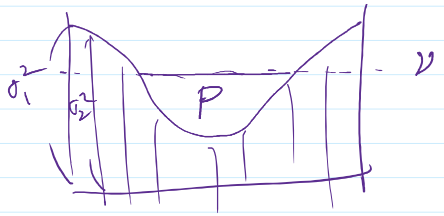

$$C\ [\text{bits/ch. use}] = \sum_{\ell=1}^{L} \log_2\left(1 + \frac{P_i}{\sigma_i^2}\right)$$

(ii) SVD

$$H = U \Sigma V^H \qquad H \in \mathbb{C}^{M\times N}$$

$U \in \mathbb{C}^{M\times M}$ $\quad UU^H = U^H U = I_M$

Σ ~~[illegible]~~ $\in \mathbb{R}^{M\times N}$ [illegible]

$H = U\Sigma V$

$U \in \mathbb{C}^{M\times M}$ $\quad UU^H = U^H U = I_M$

Σ ~~Σ~~ $\in \mathbb{R}_+^{M\times N}$, $\quad [\Sigma]_{ij} = \sigma_{ij}^2 \delta_{ij}$

$V \in \mathbb{C}^{N\times N}$ $\quad VV^H = V^H V = I_N$ $\quad \sigma_i^2 \delta_{ij}$

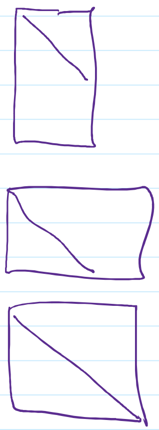

HH^H

$H^H H$ $\quad e^{j\theta_1}, e^{-j\theta_1}$ $\quad e^{-j\theta_2}$

$$H = \begin{bmatrix} 1 & & \\ & 2e^{j\theta_2} & \\ & & 3 \end{bmatrix} \quad 0$$

$$y = Hx + n = U\Sigma V^H x + n \qquad \tilde{n} = U^H n$$

$$z = U^H y = \Sigma \boxed{V^H x}_{\tilde{x}} + \tilde{n} = \Sigma \tilde{x} + \tilde{n}$$

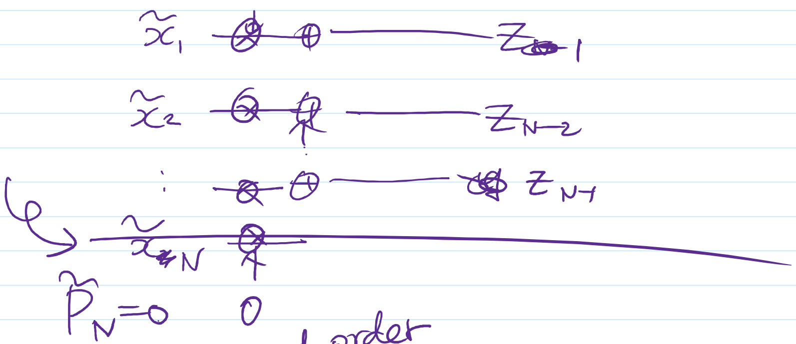

(iii) VFT

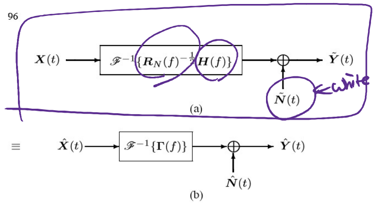

Fig. 5. (a) Conversion of the MIMO channel to an equivalent MIMO channel with vector-valued white noise. (b) Equivalent parallel MIMO channel with vector-valued white noise.

can be rewritten as $\log_2 \det\{I_{\mathcal{N}_p(f)} + \Gamma(f) R_{\hat{X}}(f) \Gamma(f)^{\mathcal{H}}\}$, where

$$R_{\hat{X}}(f) \triangleq V(f)^{\mathcal{H}} R_X(f) V(f), \tag{41}$$

and the constraint (31b) can be rewritten as $\int_{\mathcal{F}^+} \mathrm{tr}\{R_{\hat{X}}(f)\} df = P$ with a positive semi-definite matrix-valued function $R_{\hat{X}}(f)$ as the decision parameter. This implies that we now have a MIMO proper-complex Gaussian noise channel with input $\hat{X}(t)$, channel $\mathscr{F}^{-1}\{\Gamma(f)\}$, output $\hat{Y}(t)$, and average power constraint P. Therefore, from the water filling for parallel Gaussian channels, we have (38) and (40). Also by (41), we have (39). ■

We call this water filling procedure described in *Theorem 2* the cyclic water filling (CWF) because the resultant optimal input signal to the SISO channel is SOCS in general, which is proved in the following theorem.

Thus, $X_{\mathrm{opt}}(t)$ is SOCS with cycle period T. In addition, $X_{\mathrm{opt}}(t)$ is Gaussian as shown in *Theorem 2*. Moreover, by *Proposition 3*, any optimal solution to (31) with $K > 1$ is also an optimal solution to the problem with $K = 1$, which means the cycle period of an optimal solution $X_{\mathrm{opt}}(t)$ is T_0. Therefore, the conclusion follows. ■

Note that this theorem does not claim that the optimal input signal $X_{\mathrm{opt}}(t)$ cannot be second-order stationary. It can be second-order stationary, because a second-order stationary process is also an SOCS process for any cycle period $T > 0$. Note also that the optimal input is in general improper-complex. However, as it is shown in [24] and can be seen easily, the optimal input is always proper-complex if the SOCS complex Gaussian noise is proper.

V. Discussions and Numerical Results

In this section, we provide discussions and numerical results. First, we outline the proof that the worst-case interference is Gaussian given the second-order properties of the SOCS interference. By taking the Nyquist-rate samples from the output of the equivalent MIMO channel in Fig. 5 with a vector-valued white noise, the problem can be converted to a mutual information game over a discrete-time memoryless channel [22], [23]. If B_0 is an integer multiple of $1/(2T_0)$, then the result in [22, *Lemma 1*] is directly applicable to the sampled output of the equivalent channel in Fig. 5-(a) to show the Gaussianity of the worst-case interference. Otherwise, the result in [23] combined with the independence bound and

☐ $N(t)$ is second-order improper-complex cyclostationary Gaussian RP w/ cycle period $T > 0$.

☐ ((G)) $X(t)$ is a second-order improper-complex CWSCS RP w/ " " $T > 0$

Q. How can we stationarize $X(t)$?

A? FRESH vectorizer ~~VFT~~ modified? FREquency shift.

parallel Gaussian channels, we have (38) and (40). Also by (41), we have (39). ■

We call this water filling procedure described in *Theorem 2* the cyclic water filling (CWF) because the resultant optimal input signal to the SISO channel is SOCS in general, which is proved in the following theorem.

Theorem 3: The optimal input to the SOCS Gaussian noise channel is an SOCS Gaussian random process with the same cycle period as the noise.

Proof: Let $X_{l,\mathrm{opt}}(t)$ be the lth entry of the optimal input $\boldsymbol{X}_{\mathrm{opt}}(t)$ to the equivalent MIMO channel. Then, as (19), the optimal input $X_{\mathrm{opt}}(t)$ to the SISO channel can be written as

$$X_{\mathrm{opt}}(t) = \sum_{l=1}^{L} \left\{ X_{l,\mathrm{opt}}(t) e^{\mathrm{j}2\pi f_l t} + \left(X_{L+l,\mathrm{opt}}(t) e^{\mathrm{j}2\pi f_l t} \right)^* \right\}. \quad (42)$$

Now, the auto-correlation function $r_{X,\mathrm{opt}}(t,s) \triangleq \mathbb{E}\{X_{\mathrm{opt}}(t) X_{\mathrm{opt}}(s)^*\}$ of $X_{\mathrm{opt}}(t)$ can be written as

$$r_{X,\mathrm{opt}}(t,s) = \sum_{l=1}^{L} \sum_{l'=1}^{L} \Big\{ [\boldsymbol{r}_{\boldsymbol{X},\mathrm{opt}}(t-s)]_{l,l'} e^{\mathrm{j}2\pi(f_l t - f_{l'} s)} + \left([\boldsymbol{r}_{\boldsymbol{X},\mathrm{opt}}(t-s)]_{L+l,L+l'} \right)^* e^{-\mathrm{j}2\pi(f_l t - f_{l'} s)} \Big\} \quad (43a)$$

$$= r_{X,\mathrm{opt}}(t+T, s+T), \forall t, \forall s, \quad (43b)$$

where we used the fact that, by (15b), $f_l T$ and $f_{l'} T$ are always integers for all l and l', and that the optimal input $\boldsymbol{X}_{\mathrm{opt}}(t)$ has a vanishing complementary auto-correlation function. Similarly, the complementary auto-correlation function $\tilde{r}_{X,\mathrm{opt}}(t,s) \triangleq \mathbb{E}\{X_{\mathrm{opt}}(t) X_{\mathrm{opt}}(s)\}$ of $X_{\mathrm{opt}}(t)$ can be written as

$$\tilde{r}_{X,\mathrm{opt}}(t,s) = \sum_{l=1}^{L} \sum_{l'=1}^{L} \Big\{ [\boldsymbol{r}_{\boldsymbol{X},\mathrm{opt}}(t-s)]_{l,L+l'} e^{\mathrm{j}2\pi(f_l t - f_{l'} s)} + \left([\boldsymbol{r}_{\boldsymbol{X},\mathrm{opt}}(t-s)]_{L+l,l'} \right)^* e^{-\mathrm{j}2\pi(f_l t - f_{l'} s)} \Big\} \quad (44a)$$

$$= \tilde{r}_{X,\mathrm{opt}}(t+T, s+T), \forall t, \forall s. \quad (44b)$$

a mutual information game over a discrete-time memoryless channel [22], [23]. If B_0 is an integer multiple of $1/(2T_0)$, then the result in [22, *Lemma 1*] is directly applicable to the sampled output of the equivalent channel in Fig. 5-(a) to show the Gaussianity of the worst-case interference. Otherwise, the result in [23] combined with the independence bound and the water-filling argument [21] can be applied to each output branch of the equivalent channel in Fig. 5-(b).

Second, we discuss how to handle the cases with an improper-complex SOCS noise having a non-zero offset between the center frequency of symmetry and the center frequency of the communication channel. So far, it is assumed that they are the same. Unlike a proper-complex SOCS noise, an improper-complex SOCS noise exhibits non-zero spectral correlation not only between the components that are integer multiples of the symbol rate $1/T$ apart but also between two components that are equally distant from the center frequency. Thus, a real bandpass noise that is down-convertible to an improper-complex SOCS random process no longer results in an SOCS complex envelope if a different center frequency is chosen for the down-conversion. Suppose that there is a non-zero offset between these two center frequencies. Then, to make the output of the p-FRESH vectorizer a proper-complex vector-WSS random process, we need to choose the center frequency of symmetry as the origin in complex baseband. If we choose B to include the entire communication channel as before, then the interval $f \in [-B, B)$ may include a frequency band that is not a part of the communication channel. So, we need to set the channel response $H(f)$ and the interference component in the 2-D PSDs $R_N(f,f')$ and $\tilde{R}_N(f,f')$ to zero outside the communication channel, before performing the CWF.

Next, we discuss how to handle the cases with unequal frequency bands for signal transmission and reception. Suppose that the frequency bands for signal transmission and reception are overlapping but not identical. Then, we need

to re-define the frequency band for transmission as described in [20, Section III-B] and set the channel response $H(f)$ to zero outside this transmit band, before performing the CWF or possibly the modified CWF discussed above.

Next, we provide numerical results that demonstrate the effectiveness of the CWF in exploiting the cyclostationarity of the noise. For simplicity, it is assumed that the interference $N_I(t)$ is modeled as (9), where the data sequences $(c_1[n])_n$ and $(c_2[n])_n$ are independent, each data sequence consists of independent and identically distributed zero-mean real Gaussian random variables with variance σ_i^2 for $i = 1, 2$, and the transmit pulses satisfy the relation $p_1(t) = p(t)$ and $p_2(t) = p(t - \Delta)$. In what follows, the variance σ_i^2 and the offset Δ are chosen as $\sigma_2^2 = 0$ for DSB, SSB, and VSB PAMs, $\sigma_1^2 = \sigma_2^2$ and $\Delta = 0$ for QAM, and $\sigma_1^2 = \sigma_2^2$ but $\Delta = T_0/2$ for SQPSK. Let $\boldsymbol{p}(f)$ and $\hat{\boldsymbol{p}}(f)$ be the responses of the p-FRESH vectorizer to the inputs $p(t)$ and $\mathrm{j}p(t - \Delta)$. Then, it can be shown that the PSD matrix $\boldsymbol{R}_{N_I}(f)$ of $N_I(t)$ is given by

$$\boldsymbol{R}_{N_I}(f) = \frac{\sigma_1^2}{T_0} \boldsymbol{p}(f) \boldsymbol{p}(f)^{\mathcal{H}} + \frac{\sigma_2^2}{T_0} \hat{\boldsymbol{p}}(f) \hat{\boldsymbol{p}}(f)^{\mathcal{H}}, \quad (45)$$

under this assumption. Note that $\Delta = 0$ does not imply $\hat{\boldsymbol{p}}(f) = \mathrm{j}\boldsymbol{p}(f)$ in general, because the p-FRESH vectorizer is not a linear but a linear-conjugate linear operator. It can be also shown that $N_I(t)$ is proper-complex if and only if $\boldsymbol{R}_{N_I}(f)$ is a block diagonal matrix in which each block is $(\mathcal{N}_p(f)/2)$-by-$(\mathcal{N}_p(f)/2)$ for all $f \in \mathcal{F}^+$.

A root raised-cosine (RRC) pulse with roll-off factor $\beta \in [0, 1]$ is used as $p(t)$ except the SSB and the VSB modulations, where its filtered version is used instead. In addition to the bandwidth assumption (12a), $H(f)$ is assumed to be unity on the frequency band $[-B_0, B_0)$, where the bandwidth B_0 and the roll-off factor β are related to the cycle period T_0 as

$$B_0 T_0 = \frac{1+\beta}{2}, \quad (46)$$

i.e., $N_I(t)$ as well as $N_A(t)$ fully occupies the entire frequency band of interest. Under this flat channel assumption, it turns out that a result obtained by using the RRC pulse with roll-

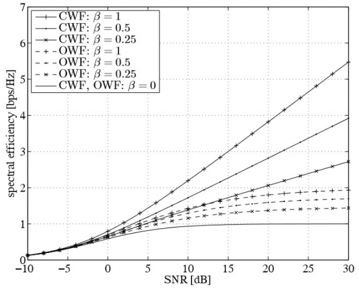

Fig. 6. Comparison of the CWF and the OWF with SIR = 0 dB when a proper-complex Gaussian interference is generated by using QAM. The same performance is observed when an improper-complex Gaussian interference is generated by using SQPSK.

a fraction $1/(WT_0) = 1/(1+\beta)$ of the frequency band and leaves $\beta/(1+\beta)$ unoccupied, as evidenced by the pre-log coefficients in (47). Fig. 6 shows the spectral efficiency C/W as functions of the signal-to-noise ratio (SNR) $P/(N_0 W)$ for various roll-off factors. The signal-to-interference ratio (SIR) P/P_I is fixed at 0 dB. Note that the CWF that exploits the spectral correlation in the cyclostationary interference significantly outperforms the OWF except the case with $\beta = 0$, where $N_I(t)$ degenerates to a proper-complex white Gaussian noise without any spectral correlation. It can be also shown that the improper-complex interference generated by using SQPSK results in the same capacity as (47). This is because, though the PSD matrix changes, its eigenvalue distribution does not change.

The second results are to compare the performance of the

Q. How can we stationarize X(t)?

A? ~~VFT~~ FRESH vectorizer modified?

FREquency shift.

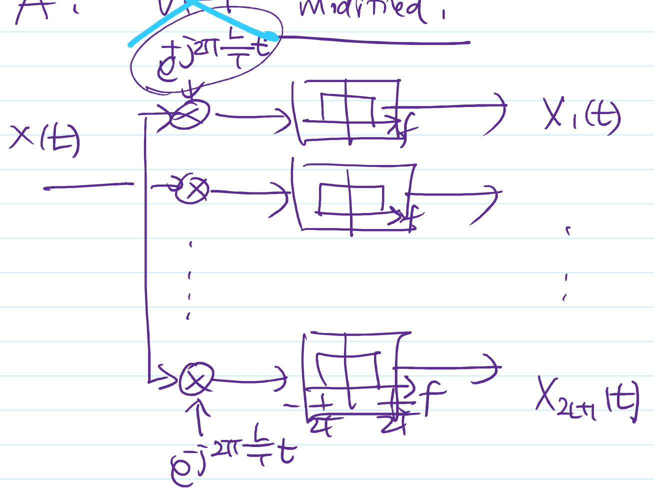

(2L+1) branches

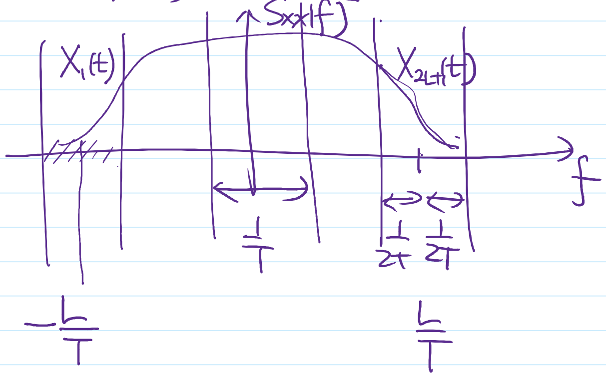

1+β.

(ex)

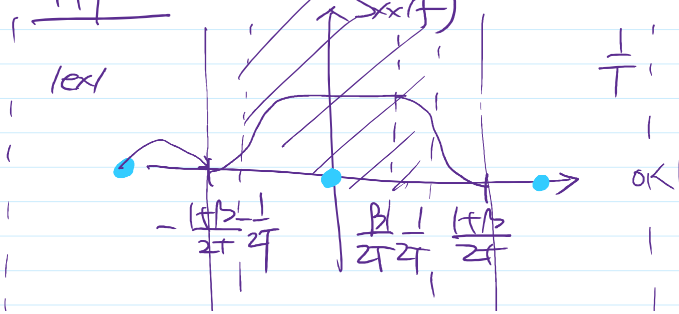

$\frac{1}{T}$

$0<\beta<1$

the roll-off factor β are related to the cycle period T_0 as

$$B_0 T_0 = \frac{1+\beta}{2}, \tag{46}$$

i.e., $N_I(t)$ as well as $N_A(t)$ fully occupies the entire frequency band of interest. Under this flat channel assumption, it turns out that a result obtained by using the RRC pulse with roll-off factor β is the same as that obtained by using any square root Nyquist pulse with excess bandwidth β. This is because, though the PSD matrix $\boldsymbol{R}_{N_I}(f)$ in (45) changes, its eigenvalue distribution does not change. For convenience, the passband bandwidth $W \triangleq 2B_0$ is used throughout this section.

The first results are to compare the performance of the CWF with that of the ordinary water filling (OWF), which ignores the spectral correlation in the cyclostationary noise $N(t)$. The interference is generated by using QAM, thus proper-complex, and leads to the power P_I. Then, it can be shown that the capacity of this SOCS proper-complex Gaussian noise channel is given by

$$C = \frac{W\beta}{1+\beta}\log_2\left(1+\frac{\min(P,\beta P_I)+\frac{[P-\beta P_I]^+\beta}{1+\beta}}{N_0\frac{W\beta}{1+\beta}}\right) + \frac{W}{1+\beta}\log_2\left(1+\frac{\frac{[P-\beta P_I]^+}{1+\beta}}{N_0\frac{W}{1+\beta}+P_I}\right)\ \text{[bps]}, \tag{47}$$

for $0 \le \beta \le 1$. This is because, though $N_I(t)$ physically occupies the entire frequency band, it occupies in effect only

noise without any spectral correlation. It can be also shown that the improper-complex interference generated by using SQPSK results in the same capacity as (47). This is because, though the PSD matrix changes, its eigenvalue distribution does not change.

The second results are to compare the performance of the CWF with that of the OWF, when the interference is generated by using DSB PAM, thus improper-complex. Since $N_I(t)$ exists only in the real part, the OWF separately processes the real and the imaginary parts. Then, it can be shown that the capacity of this SOCS improper-complex Gaussian noise channel is given by

$$C = \frac{W(1+2\beta)}{2+2\beta} \times \log_2\left(1+\frac{\min(P,(1+2\beta)P_I)+\frac{[P-(1+2\beta)P_I]^+(1+2\beta)}{2+2\beta}}{N_0\frac{W(1+2\beta)}{2+2\beta}}\right) + \frac{W}{2+2\beta}\log_2\left(1+\frac{\frac{[P-(1+2\beta)P_I]^+}{2+2\beta}}{N_0\frac{W}{2+2\beta}+P_I}\right)\ \text{[bps]}, \tag{48}$$

for $0 \le \beta \le 1$. This is because $N_I(t)$ occupies in effect only a fraction $1/(2+2\beta)$ of the frequency band and leaves $(1+2\beta)/(2+2\beta)$ unoccupied, as evidenced by the pre-log coefficients in (48). Similar to Fig. 6, Fig. 7 shows the spectral efficiency versus SNR with the SIR fixed at 0 dB. Note again that the CWF significantly outperforms the OWF except the

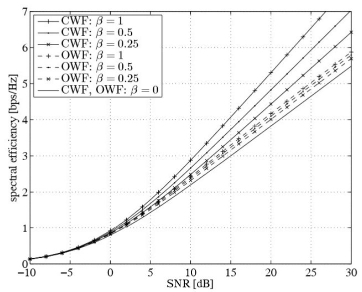

Fig. 7. Comparison of the CWF and the OWF with SIR = 0 dB when an improper-complex Gaussian interference is generated by using DSB or SSB PAM.

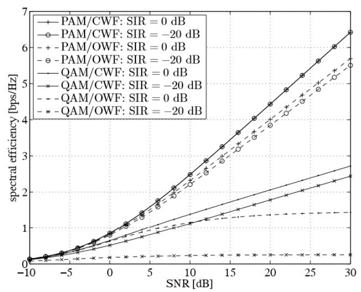

Fig. 8. Comparison of the CWF and the OWF when $\beta = 0.25$ and SIR = 0 and −20 dB.

case with $\beta = 0$, where $N_I(t)$ degenerates to a real white Gaussian noise with only impropriety to be exploited. In this case, the capacity formula (48) reduces to that for a parallel Gaussian noise channel with two sub-channels having the same bandwidth $W/2$ but different noise power $N_0W/2$ and $N_0W/2+P_I$, respectively. This result perfectly agrees with the intuition for independently processed real and imaginary parts. It can be also shown that the improper-complex interference generated by using SSB PAM results in the same capacity as (48) and, consequently, the same spectral efficiency as Fig. 7, when the channel includes the negative frequency band that is not occupied by $N_I(t)$. This is because both the DSB and the SSB PAMs utilize only half the frequency band. It is also the case with the improper-complex interference generated by using VSB PAM. To the contrary, when the channel does not includes the negative frequency band, the improper-complex interference generated by using SSB PAM results in half the channel capacity of (47) and, consequently, the same spectral efficiency as Fig. 6.

The final results are to compare the performance of the CWF with that of the OWF, when a strong interference is present in the channel. Fig. 8 shows the spectral efficiency of the channels considered in Figs. 6 and 7 versus SNR, now with $\beta = 0.25$ and SIR = 0 and −20 dB. When $N_I(t)$ is

VI. Conclusions and Future Work

In this paper, we have derived the capacity of an SOCS complex Gaussian noise channel. By using the p-FRESH vectorization of the input, the impulse response, and the output of the channel, the SISO channel is converted into an equivalent MIMO channel and its capacity is derived in the frequency domain. A geometric procedure called the CWF is proposed to construct an optimal input distribution that achieves the capacity. It is shown that the CWF significantly outperforms the OWF that ignores the spectral correlation of the SOCS noise. This result can be applied to various interference types of PAM, QAM, and their variants including the WCDMA short-code and IEEE 802.11 DS/SS signals, which have massive spectral redundancies.

Although the CWF achieves the capacity, the knowledge on the center frequency of the SOCS noise is required when the complex noise is improper. Thus, extensions to the cases with an uncertainty in the center frequency or with a channel impairment in the form of phase jittering are interesting future research directions. Deriving the capacity and the capacity-achieving schemes for a channel with a non-Gaussian noise or with multiple spectrally overlapping improper-complex SOCS interferences having different center frequencies is another future work that warrants further investigation. Particularly, in the latter case, the use of the spectral correlation density

$\frac{\beta}{2T}\ \frac{1}{2T}, \frac{1+\beta}{2T}$

$$X(t) \to \boxed{\text{VFT}} \to \underline{X}(t) = \begin{bmatrix} X_1(t) \\ X_2(t) \\ X_3(t) \end{bmatrix}$$

$f=0$, $\cancel{D=1}$ $D(0)=1$

$\frac{\beta}{2T} < |f| < \frac{1}{2T}$, $D(f)=2$

$D(f)$

$D: [-\frac{1}{2T}, \frac{1}{2T}) \to \mathbb{Z}$

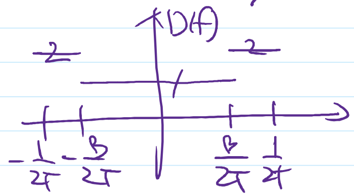

$$\frac{1}{\frac{1}{T}}\int_{-\frac{1}{2T}}^{\frac{1}{2T}} D(f)\,df = 1+\beta$$

□ p-FRESH vectorizer

↑ properizing

Q. Show

$\underline{X}(t)$ is proper!

A. It suffices to show

$E\{\underline{X}(t)\underline{X}^T(s)\} = 0 \quad \forall (t,s)$

efficiency in Fig. 8.

The final results are to compare the performance of the CWF with that of the OWF, when a strong interference is present in the channel. Fig. 8 shows the spectral efficiency of the channels considered in Figs. 6 and 7 versus SNR, now with $\beta = 0.25$ and SIR $= 0$ and -20 dB. When $N_I(t)$ is generated by DSB PAM, the CWF suffers no performance degradation. This is because the CWF at SIR $= 0$ dB orthogonalizes the channel input to the interference, so that the enhanced interference level at any SIR < 0 dB does not affect the performance at all. To the contrary, the OWF suffers performance degradation because, though most of the information transmission is through the imaginary part, it observes severe noise enhancement in the real part. When $N_I(t)$ is generated by QAM, the CWF suffers much mild performance degradation than the OWF. This is because, though severe noise enhancement is observed in all frequency components, the CWF can exploit the spectral correlation to suppress the interference.

research directions. Deriving the capacity and the capacity-achieving schemes for a channel with a non-Gaussian noise or with multiple spectrally overlapping improper-complex SOCS interferences having different center frequencies is another future work that warrants further investigation. Particularly, in the latter case, the use of the spectral correlation density function [4, Ch. 1] or its variant will be necessary to characterize the interferences in the cycle frequency and the spectral frequency domains. It is also an interesting future research to derive practical signal processing structures that provide the same properizing and stationarizing operation as the p-FRESH vectorizer.

ACKNOWLEDGMENTS

We wish to thank Dr. Shuangqing Wei, Louisiana State University, for helpful discussions. We also wish to thank anonymous reviewers and the Associate Editor for their constructive suggestions and comments.

APPENDIX

A. Proof of Lemma 1

Proof: It is straightforward to show (21a) by using $\mu_Y(t) = 0, \forall t$. To show (21b) and (21c), similar to (13a) and (13b), let $\{R_Y^{(k)}(f)\}_{k\in\mathbb{Z}}$ and $\{\tilde{R}_Y^{(k)}(f)\}_{k\in\mathbb{Z}}$ be the functions such that $R_Y(f,f') = \sum_{k=-\infty}^{\infty} R_Y^{(k)}(f-k/T)\delta(f-f'-k/T)$ and $\tilde{R}_Y(f,f') = \sum_{k=-\infty}^{\infty} \tilde{R}_Y^{(k)}(f-k/T)\delta(f-f'-k/T)$. Then, the cross-correlation between $Y_l(t)$ and $Y_{l'}(s)$ for $l, l' \le L$ is given by

$$\mathbb{E}\{Y_l(t)Y_{l'}(s)^*\} = \int_{-B}^{B}\int_{-B}^{B} G(f-f_l)e^{j2\pi(f-f_l)t}R_Y(f,f') \cdot G(f'-f_{l'})^* e^{-j2\pi(f'-f_{l'})s} df\, df' \quad (49a)$$

$$= \int_{\mathcal{F}_l^+}\int_{\mathcal{F}_{l'}^+} R_Y(f,f')e^{j2\pi(ft-f's)}e^{-j2\pi(f_lt-f_{l'}s)} df\, df' \quad (49b)$$

$$= \int_{\mathcal{F}^+} R_Y^{(l-l')}(f+f_{l'})e^{j2\pi f(t-s)} df, \quad (49c)$$

where Parseval's relation is used twice in (49a) and the identity $f_l - f_{l'} = (l-l')/T$ is used in (49c). In the same way, we have

$$\mathbb{E}\{Y_l(t)Y_{l'}(s)^*\} = \begin{cases} \int_{\mathcal{F}^+} \tilde{R}_Y^{(l-l'+L)}(f+f_{l'-L})e^{j2\pi f(t-s)}df, & \text{for } l \le L < l', \\ \int_{\mathcal{F}^+} \tilde{R}_Y^{(l'-l+L)}(-f-f_{l'})^* e^{j2\pi f(t-s)}df, & \text{for } l' \le L < l, \\ \int_{\mathcal{F}^+} R_Y^{(l'-l)}(-f-f_{l'-L})^* e^{j2\pi f(t-s)}df, & \text{for } l, l' > L. \end{cases} \quad (50)$$

Thus, the cross-correlation $\mathbb{E}\{Y_l(t)Y_{l'}(s)^*\}$ becomes a function only of $t-s, \forall l, \forall l'$.

On the other hand, the complementary cross-correlation between $Y_l(t)$ and $Y_{l'}(s)$ for $l, l' \le L$ is given by

$$\mathbb{E}\{Y_l(t)Y_{l'}(s)\} = \int_{-B}^{B}\int_{-B}^{B} G(f-f_l)e^{j2\pi(f-f_l)t}\tilde{R}_Y(f,-f') \cdot G(f'-f_{l'})e^{j2\pi(f'-f_{l'})s} df\, df' \quad (51a)$$

$$= \int_{\mathcal{F}_l^+}\int_{\mathcal{F}_{l'}^+} \tilde{R}_Y(f,-f')e^{j2\pi(f-f_l)t}e^{j2\pi(f'-f_{l'})s} df\, df' \quad (51b)$$

$$= 0. \quad (51c)$$

This is because the impulse fences of $\tilde{R}_Y(f,-f')$ on $f = -f' - m/T$ do not cross the integration area $(f, f') \in \mathcal{F}_l^+ \times \mathcal{F}_{l'}^+$. In the same way, we have $\mathbb{E}\{Y_l(t)Y_{l'}(s)\} = 0$ for other cases of l, l'. Thus, the complementary cross-correlation $\mathbb{E}\{Y_l(t)Y_{l'}(s)\}$ becomes zero, $\forall l, \forall l'$. Therefore, the conclusion follows. ■

B. Proof of Lemma 2

Proof: The Hermitian symmetry follows straightforwardly from the element-wise Fourier transform of $r_{\boldsymbol{X}}(\tau) =$

LTI filter output sampled at $t = 0$ is given by

$$\mathbb{E}\left\{\left\|\boldsymbol{A}(-t)^{\mathcal{H}} * \boldsymbol{Y}(t)|_{t=0}\right\|^2\right\}$$

$$= \sum_{l=1}^{2L}\sum_{l'=1}^{2L}\int_{-\infty}^{\infty}\int_{-\infty}^{\infty} a_l(\tau)^*[\boldsymbol{r_Y}(\tau,\tau')]_{l,l'}a_{l'}(\tau')d\tau d\tau' \quad (52a)$$

$$= \sum_{l=1}^{2L}\sum_{l'=1}^{2L}\int_{\mathcal{F}^+} A_l(f)^*[\boldsymbol{R_Y}(f)]_{l,l'}A_{l'}(f)df \quad (52b)$$

$$= \int_{\mathcal{F}^+} \boldsymbol{a}(f)^{\mathcal{H}}\boldsymbol{R_Y}(f)\boldsymbol{a}(f)df \ge 0, \quad (52c)$$

where $\boldsymbol{a}(f)$ is the $2L$-by-1 vector of the element-wise Fourier transform of $[a_1(t), a_2(t), ..., a_{2L}(t)]^{\mathcal{T}}$. Since $a_l(t)$ is arbitrary for all l, (52c) implies $\boldsymbol{a}(f)^{\mathcal{H}}\boldsymbol{R_Y}(f)\boldsymbol{a}(f) \ge 0, \forall \boldsymbol{a}(f), \forall f \in \mathcal{F}^+$. Therefore, the conclusion follows. ■

REFERENCES

[1] W. C. Y. Lee, *Wireless & Cellular Telecommunicaions*, 3rd edition. McGraw Hill, 2006.
[2] W. R. Bennett, "Statistics of regenerative digital transmissions," *Bell Syst. Tech. J.*, vol. 37, no. 6, pp. 1501–1542, Nov. 1958.
[3] J. G. Proakis, *Digital Communications*, 4th edition. McGraw Hill, 2001.
[4] W. A. Gardner, editor, *Cyclostationarity in Communications and Signal Processing*. IEEE Press, 1994.
[5] E. Serpedin, F. Panduru, I. Sar, and G. B. Giannakis, "Bibliography on cyclostationarity," *Signal Process.*, vol. 85, no. 12, pp. 2233–2303, Dec. 2005.
[6] W. A. Gardner, A. Napolitano, and L. Paura, "Cyclostationarity: half a century of research," *Signal Process.*, vol. 86, no. 4, pp. 639–697, Apr. 2006.
[7] C. M. Spooner and W. A. Gardner, "The cumulant theory of cyclostationary time-series, part II: development and applications," *IEEE Trans. Signal Process.*, vol. 42, no. 12, pp. 3409–3429, Dec. 1994.
[8] A. Punchihewa, Q. Zhang, O. A. Dobre, C. Spooner, S. Rajan, and R. Inkol, "On the cyclostationarity of OFDM and single carrier linearly digitally modulated signals in time dispersive channels: theoretical developments and application," *IEEE Trans. Wireless Commun.* vol. 9, no. 8, pp. 2588–2599, Aug. 2010.
[9] W. A. Gardner and L. E. Franks, "Characterization of cyclostationary random signal processes," *IEEE Trans. Inf. Theory*, vol. 21, no. 1, pp. 4–14, Jan. 1975.
[10] D. A. Shnidman, "A generalized Nyquist criterion and an optimum linear receiver for a pulse modulation system," *Bell Syst. Tech. J.*, vol. 46, no. 9, pp. 2163–2177, Nov. 1967.
[11] J. R. Barry, E. A. Lee, and D. G. Messerschmitt, *Digital Communication*, 3rd edition. Kluwer Academic Publishers, 2004.
[12] T. Berger and D. W. Tufts, "Optimum pulse amplitude modulation–part I: transmitter-receiver design and bounds from information theory," *IEEE Trans. Inf. Theory*, vol. 13, no. 2, pp. 196–208, Apr. 1967.
[13] J. Yang and S. Roy, "On joint transmitter and receiver optimization for multiple-input-multiple-output (MIMO) transmission systems," *IEEE Trans. Commun.*, vol. 42, no. 12, pp. 3221–3231, Dec. 1994.
[14] H. S. Mir and S. Roy, "Optimum transmitter/receiver design for a narrowband overlay in noncoordinated subscriber lines," *IEEE Trans. Commun.*, vol. 52, no. 6, pp. 992–998, June 2004.
[15] J. H. Cho and W. Gao, "Continuous-time equivalents of Welch bound equality sequences," *IEEE Trans. Inf. Theory*, vol. 51, no. 9, pp. 3176–3185, Sep. 2005.
[16] J. H. Cho, "Multi-user constrained water-pouring for continuous-time overloaded Gaussian multiple-access channels," *IEEE Trans. Inf. Theory*, vol. 54, no. 4, pp. 1437–1459, Apr. 2008.
[17] W. A. Gardner, "Cyclic Wiener filtering: theory and method," *IEEE Trans. Commun.*, vol. 41, no. 1, pp. 151–163, Jan. 1993.
[18] Y. C. Eldar, "Uncertainty relations for shift-invariant analog signals," *IEEE Trans. Inf. Theory*, vol. 55, no. 12, pp. 5742–5757, Dec. 2009.

F, ... shifted ... is shown

$E\{X(t)X^T(s)\} = 0 \quad \forall (t,s)$

☐ Why?

$x(t)$ a real-valued signal of finite energy

$X(f)$ CTFT of $x(t)$

$$X(f) = \int_{-\infty}^{\infty} x(t)e^{-j2\pi ft}dt$$
$$= \int_{-\infty}^{\infty} x^*(t)e^{-j2\pi ft}dt$$
$$= \left(\int_{-\infty}^{\infty} x(t)e^{j2\pi ft}dt\right)^*$$
$$= \{X(-f)\}^*$$
$$= X^*(-f), \quad \forall f$$

$x(t) = x^*(t), \forall t$

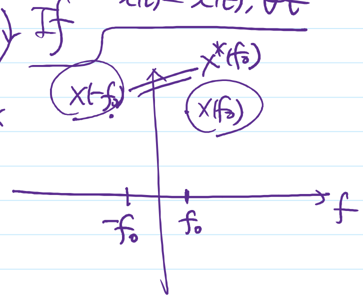

☐ Improper-Complex RP

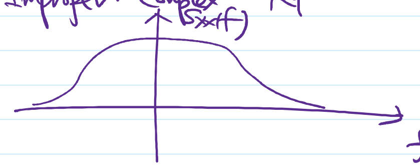

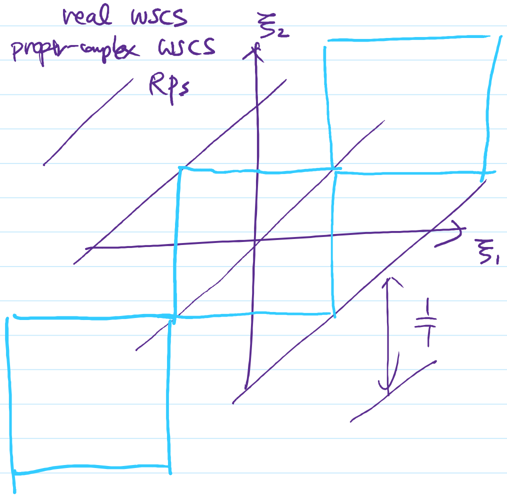

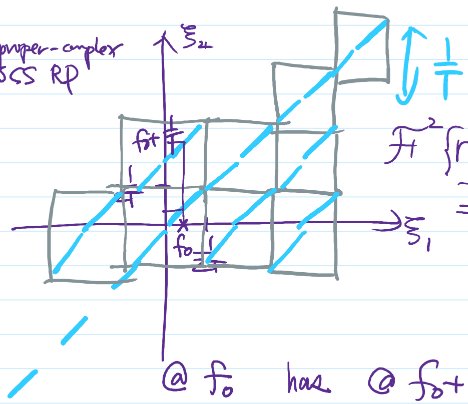

$\mathcal{F}^2\{r_{xx}(t,s)\} = E\{X(t)X^*(s)\}$

@ f_0 has @ $f_0 + \frac{\ell}{T}$

sion follows. ∎

B. Proof of Lemma 2

Proof: The Hermitian symmetry follows straightforwardly from the element-wise Fourier transform of $\boldsymbol{r}_{\boldsymbol{Y}}(\tau) = \mathbb{E}\{\boldsymbol{Y}(t)\boldsymbol{Y}(t-\tau)^{\mathcal{H}}\} = \mathbb{E}\{\boldsymbol{Y}(t-\tau)\boldsymbol{Y}(t)^{\mathcal{H}}\}^{\mathcal{H}} = \boldsymbol{r}_{\boldsymbol{Y}}(-\tau)^{\mathcal{H}}$. Now, consider filtering the p-FRESH vectorizer output $\boldsymbol{Y}(t)$ by using the LTI filter with impulse response $\boldsymbol{A}(-t)^{\mathcal{H}} \triangleq \mathrm{diag}\{a_1(-t)^*, a_2(-t)^*, ..., a_{2L}(-t)^*\}$. Then, the power of the

[16] J. H. Cho, "Multi-user constrained water-pouring for continuous-time overloaded Gaussian multiple-access channels," *IEEE Trans. Inf. Theory*, vol. 54, no. 4, pp. 1437–1459, Apr. 2008.

[17] W. A. Gardner, "Cyclic Wiener filtering: theory and method," *IEEE Trans. Commun.*, vol. 41, no. 1, pp. 151–163, Jan. 1993.

[18] Y. C. Eldar, "Uncertainty relations for shift-invariant analog signals," *IEEE Trans. Inf. Theory*, vol. 55, no. 12, pp. 5742–5757, Dec. 2009.

[19] J. H. Cho, "Joint transmitter and receiver optimization in additive cyclostationary noise," *IEEE Trans. Inf. Theory*, vol. 50, no. 14, pp. 3396–3405, Dec. 2004.

[20] Y. H. Yun and J. H. Cho, "An optimal orthogonal overlay for a cyclostationary legacy signal," *IEEE Trans. Commun.*, vol. 58, no. 5, pp. 1557–1567, May 2010.

[21] T. M. Cover and J. A. Thomas, *Elements of Information Theory*, 2nd edition. John Wiley & Sons, Inc., 2006.

[22] C. R. Baker and I. -F. Chao, "Information capacity of channels with partially unknown noise, I: finite-dimensional channels," *SIAM J. Appl. Math.*, vol. 56, no. 3, pp. 946–963, June 1996.

[23] N. M. Blachman, "Communication as a game," in *Proc. 1957 IRE WESCON Conf. Rec.*, vol. 2, pp. 61–66.

[24] B. W. Han and J. H. Cho, "Cyclic water filling for additive wide-sense cyclostationary Gaussian noise channel," in *Proc. 2009 Inf. Theory Applications Workshop*.

[25] D. Tse and P. Viswanath, *Fundamentals of Wirelss Communication*. Cambridge Univ. Press, 2005.

[26] A. Goldsmith, *Wireless Communications*. Cambridge Univ. Press, 2005.

[27] F. D. Neeser and J. L. Massey, "Proper complex random processes with applications to information theory," *IEEE Trans. Inf. Theory*, vol. 39, no. 4, pp. 1293–1302, July 1993.

[28] B. Picinbono and P. Bondon, "Second-order statistics of complex signals," *IEEE Trans. Signal Process.*, vol. 45, no. 2, pp. 411–420, Feb. 1997.

[29] P. Wahlberg and P. J. Schreier, "Spectral relations for multidimentional complex improper stationary and (almost) cyclostationary processes," *IEEE Trans. Inf. Theory*, vol. 54, no. 4, pp. 1670–1682, Apr. 2008.

[30] W. Gardner and W. Brown, "Frequency-shift filtering theory for adaptive co-channel interference removal," in *Proc. 1989 Asilomar Conf. Signals, Systems, Computers*, vol. 2, pp. 562–567.

[31] B. Agee, "Solving the near-far problem: exploitation of spectral and spatial coherence in wireless personal communication networks," in *Proc. 1993 Virginia Tech Symp. Wireless Pers. Commun.*, pp. 15-1 – 15-12.

[32] U. Madhow and M. Honig, "On the average near-far resistance for MMSE detection of direct-sequence CDMA signals with random spreading," *IEEE Trans. Inf. Theory*, vol. 45, no. 6, pp. 2039–2045, Sep. 1999.

[33] W. M. Brown, "Conjugate linear filtering," *IEEE Trans. Inf. Theory*, vol. 15, no. 4, pp. 462–465, July 1969.

[34] B. Picinbono and P. Chevalier, "Widely linear estimation with complex data," *IEEE Trans. Signal Process.*, vol. 43, no. 8, pp. 2030–2033, Aug. 1995.

Byung Wook Han received the B.S. degree in electrical engineering in 2004 from Pohang University of Science and Technology (POSTECH), Pohang, Korea, where he is currently working toward the Ph.D. degree. His research interests include information theory and multiuser communications.

Joon Ho Cho (S'99-M'01) received the B.S. degree (summa cum laude) in electrical engineering from Seoul National University, Seoul, Korea, in 1995, and the M.S.E.E. and Ph.D. degrees in electrical and computer engineering from Purdue University, West Lafayette, IN, in 1997 and 2001, respectively.

From 2001 to 2004, he was with the University of Massachusetts at Amherst as an Assistant Professor. Since July 2004, he has been with Pohang University of Science and Technology (POSTECH), Pohang, Korea, where he is presently an Associate Professor in the Department of Electrical Engineering. His research interests include wideband systems, multiuser communications, adaptive signal processing, channel measurement and modeling, and information theory.

Dr. Cho has served as an Associate Editor for the IEEE Transactions on Vehicular Technology.

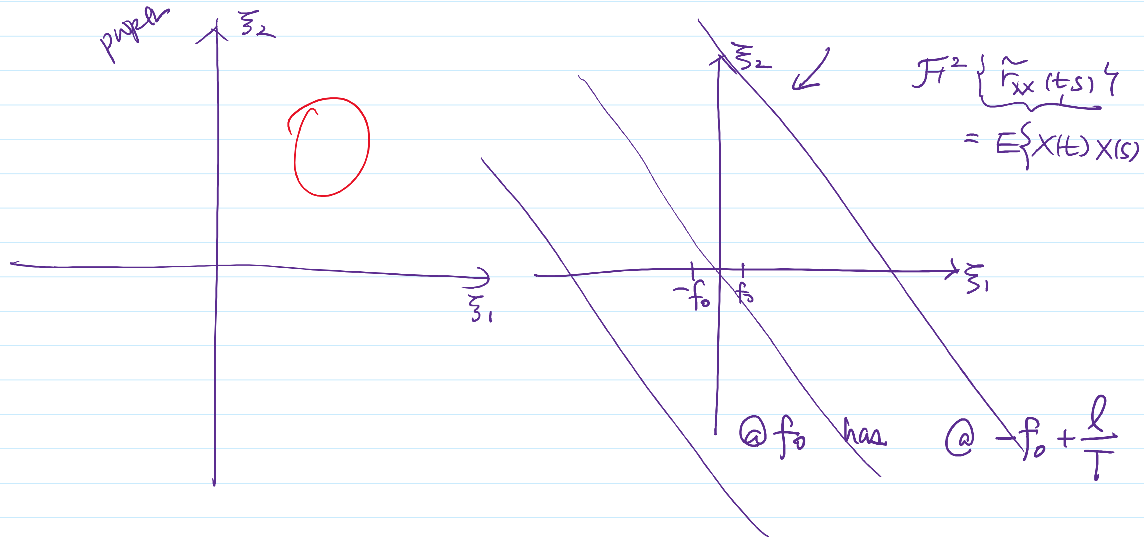

$\mathcal{F}^2\{\underbrace{\tilde{r}_{xx}(t,s)}\}$

$= E\{X(t)X(s)\}$